



**Intelligent Information System Supporting  
Observation, Searching and Detection for  
Security of Citizens in Urban Environment**



European Seventh Framework Programme  
FP7-218086-Collaborative Project

## Deliverable 2.5. Proposed algorithms and methods for autonomous steering and navigation of UAVs

### **The INDECT Consortium**

AGH — University of Science and Technology, AGH, Poland  
Gdansk University of Technology, GUT, Poland  
InnoTec DATA GmbH & Co. KG, INNOTECH, Germany  
IP Grenoble (Ensimag), INP, France  
MSWiA — General Headquarters of Police (Polish Police), GHP, Poland  
Moviquity, MOVIQUITY, Spain  
Products and Systems of Information Technology, PSI, Germany  
Police Service of Northern Ireland, PSNI, United Kingdom  
Poznan University of Technology, PUT, Poland  
Universidad Carlos III de Madrid, UC3M, Spain  
Technical University of Sofia, TU-SOFIA, Bulgaria  
University of Wuppertal, BUW, Germany  
University of York, UoY, Great Britain  
Technical University of Ostrava, VSB, Czech Republic  
Technical University of Kosice, TUKE, Slovakia  
X-Art Pro Division G.m.b.H., X-art, Austria  
Fachhochschule Technikum Wien, FHTW, Austria

©Copyright 2010, the Members of the INDECT Consortium



## Document Information

<b>Contract Number</b>	218086
<b>Deliverable Name</b>	Proposed algorithms and methods for autonomous steering and navigation of UAVs
<b>Deliverable number</b>	Deliverable 2.5.
<b>Editor(s)</b>	Paweł Lubarski, PUT
<b>Author(s)</b>	Paweł Lubarski, PUT Krzysztof Witkowski, PUT Wojciech Mruczkiewicz, PUT Mikołaj Szłapka, PUT Mateusz Nawrocki, PUT Błażej Sołtowski, PUT Piotr Domagalski, PUT
<b>Reviewer(s)</b>	Maciej Gucma, PhD, Maritime University of Szczecin
<b>Dissemination level</b>	public
<b>Contractual date of delivery</b>	30-06-2010
<b>Delivery date</b>	30-06-2010
<b>Status</b>	v. 1.0
<b>Keywords</b>	tracking, positioning, control, navigation, UAV



This project is funded under 7<sup>th</sup> Framework Program



# Contents

<b>Document Information</b>	<b>3</b>
<b>Executive Summary</b>	<b>7</b>
<b>Introduction</b>	<b>9</b>
<b>1 Overview</b>	<b>11</b>
1.1 Use cases	11
1.2 Requirements	11
1.2.1 Endurance	11
1.2.2 Construction	11
1.2.3 Optical gimbal	12
1.2.4 Control	12
<b>2 Mechanical design</b>	<b>12</b>
2.1 Burzyk UAV - components.	12
2.1.1 The Engine	12
2.1.2 The Wing	14
2.1.3 The Stabilizer	14
2.1.4 The Fuselage	14
2.2 Launch systems	15
2.2.1 Wheels	15
2.2.2 Catapult	15
2.2.3 Hand	15
2.3 Summary	15
<b>3 Control</b>	<b>17</b>
3.1 Equations of Motion	17
3.2 System Identification	19
3.3 Control Algorithms Overview	21
3.4 PID Controllers	22
3.4.1 Pitch Hold	22
3.4.2 Altitude Hold	22
3.4.3 Roll Hold	23
3.4.4 Coordinated Turn	23
3.4.5 Heading Hold	23
3.4.6 Automatic Landing	24
<b>4 Localization</b>	<b>24</b>
4.1 Overview	24
4.2 GPS	24
4.2.1 Principles of Operation	25
4.2.2 Performance of Stand-Alone GPS	26
4.2.3 Augmentations	27
4.3 IMU	27
4.3.1 Overview	27
4.3.2 Accelerometers	27
4.3.3 Gyroscopes	28
4.3.4 Inclinometer	28
4.4 Magnetic sensors	28
4.4.1 Overview	28
4.4.2 Errors and performance	29
4.5 Aerometric sensors	29
4.5.1 Overview	29
4.5.2 Errors and performance	30

---

4.6	Filtering . . . . .	30
4.6.1	Kalman Filter overview . . . . .	30
4.6.2	The discrete-time Kalman filter algorithm . . . . .	30
4.6.3	Extended Kalman Filter . . . . .	31
4.6.4	Unscented Kalman Filter . . . . .	32
<b>5</b>	<b>Navigation</b>	<b>32</b>
5.1	Overview . . . . .	32
5.2	Missile guidance laws . . . . .	32
5.3	Linear proportional–integral–derivative controller (PID) trajectory tracking . . .	33
5.4	Non-linear guidance logic for trajectory tracking . . . . .	33
<b>6</b>	<b>Future work</b>	<b>35</b>
	<b>Conclusions</b>	<b>35</b>

## Executive Summary

In this document we describe proposed solutions and algorithms which will be used in the UAV.

In Section 1 a general view of the document is given. It also describes briefly user feedback we had.

Section 2 provides draft preliminary design of the UAV which is described including launch system.

Section 3 describes equations of motion and control algorithms, which will be used by the UAV.

Localization sensors and methods of using this data to optimally compute position of the UAV is provided in Section 4.

Methods of path following and navigation are described in Section 5.

The document is concluded in Section 6 with a summary of future work to be done.



## Introduction

Task 2.5 in work package WP2 concerns two main parts: development of a autonomous UAV and development of an advanced observation system.

This document is focused on the first area of development in this task. To complete this task all important modules must be described.

UAV consists of mechanical elements described in Section 2. Apart of that software must be developed. We have decided to create a 3 layer system - mission, navigation and control. Control is described in Section 3, localization and navigation in Sections 4 and 5. Mission planning of a single UAV is described in deliverable 2.6.

Therefore at this moment reader of both deliverables will have a full overview of planned development of UAV.



# 1. Overview

In the following deliverable we have worked on algorithms and methods for autonomous steering and navigation of UAVs. In order to discuss specific algorithms and methods we had to create an UAV that fulfills the end-user requirements and meets their expectations. In the first step we have shown our previous UAVs and their properties to the end-users. We also asked them to fill in the documents that we created - user scenarios and technical tactical requirements. These document templates can be found in attachment number 1. Thanks to these documents we have proposed the light UAV and the end-users agreed that this solution will be sufficient for their needs. In the first chapter we wrote in general about the use cases and requirements, since the scenarios and technical tactical requirements are confidential and available only for the consortium members. In the following chapters we have described the mechanical design, control methods, localization and navigation algorithms.

## 1.1. Use cases

After analyzing the end-user requirements, their use case scenarios and having discussed couple of propositions we have decided to create a light UAV.

- It will be used to monitor covertly and overtly terrain, people and property in urban and rural environment. The onboard algorithms will allow to track the desired objects and estimate their positions for example if a car goes through a tunnel or hides behind trees.
- The UAV has to be quite small and it should be constructed in a way that allows fast assembly. One of the main requirements is that it will be transported by car or in a backpack and assembled near the mission area.
- It will not require a runway or any other infrastructure, except the equipment brought in a car or a backpack.
- The UAV could be used to monitor the border, in search and rescue missions, to scout the mission area etc.

## 1.2. Requirements

After consultation with end users we have decided to create a system that will meet these requirements:

### 1.2.1. Endurance

**Flight time** 2h

**Communication Range** 5km

**Maximum height** 500m

### 1.2.2. Construction

- Easy to assemble.
- Fast to assemble in field. (Assembly time lower than 15 min.)
- Robust

### 1.2.3. Optical gimbal

- Should be easily replaced

Available payloads:

- Thermal vision
- Motor zoom
- Focal length Daylight

Image should be saved onboard

### 1.2.4. Control

- Autonomous – no need for operator to control the state of UAV.
- Possible changes of mission during flight.
- Possible tracking of objects based on visual identification.

Possible modes of operation based on energy consumption:

- normal – optimal energy usage;
- low-power – for extending standard endurance, or used in difficult situations;
- hi-power – for short, but intensive operations;

## 2. Mechanical design

This chapter describes the construction of the Burzyk UAV, that is constructed within the tasks of INDECT project. All main parts of the plane are briefly discussed here. Also the main rationale of the hardware choices are given.

The dimensions of the UAV are 1650 mm length and 2400 mm of wingspan. The total weight of the plane equipped with the gimbal, battery and the electronic elements is about 6 kg. The start is carried out by throwing the UAV by hand, catapult or from the launching cart. It is propelled by electric motor, which enables to achieve appropriate altitude and ensures the safe flight for the whole operation time.

Burzyk has been constructed in the way that allows to pack it into special backpack after decomposition. Due to that feature the fast and easy transport from one place to another is possible. There is huge variety of applications for Burzyk. Beginning from observation of the forests, even to the military operations. The only problem is to find the appropriate place for assembly and take off. Its little size together with silent engine and volplane option make Burzyk an ideal plane to use in the scientific and industrial field. Figure 1 presents the overview of Burzyk.

### 2.1. Burzyk UAV - components.

#### 2.1.1. The Engine

The choice of the engine for Burzyk was based on a few criteria. Many different types of future tasks had to be taken into account. After analysis of all requirements the constructors decided that the engine must be “silent”, but with enough power to go up quickly and safely to the desired altitude and ensure safe and stable flight. The next criterion was the size. We chose the electric 700W engine, which meets all mentioned above requirements. The internal combustion engine was inapplicable because of the larger dimensions and high loudness in comparison to electric one. Another advantage of the electric engine is possibility of switching it off and on during the flight. Such a feature enables volplane and extends the possible duration of the flight. The engine is placed in the upper part of the UAV, what is shown in the 2.

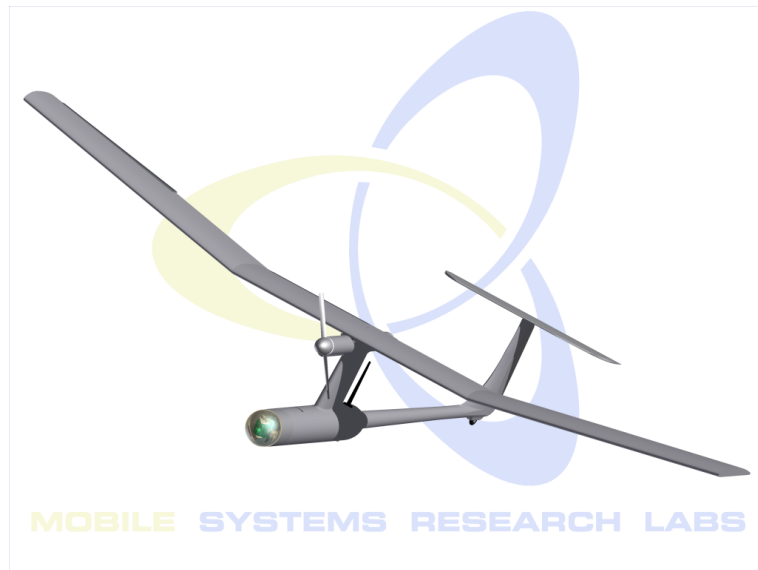


Figure 1: Burzyk overview

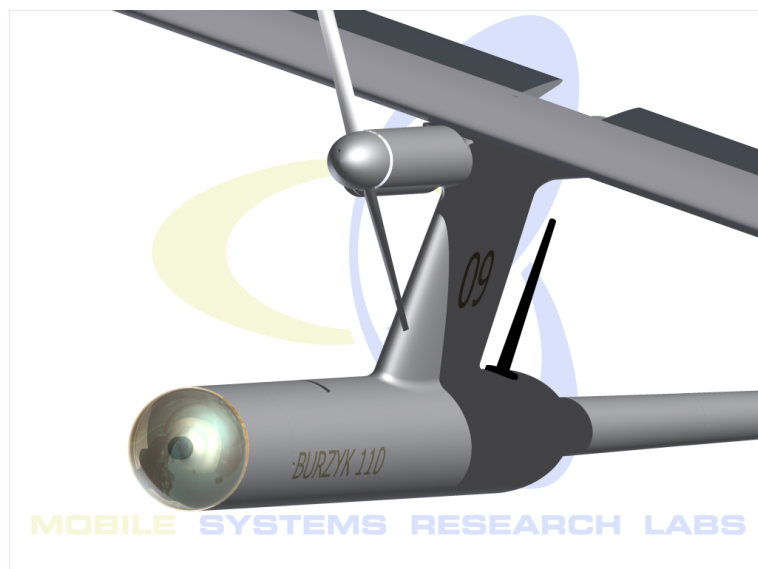


Figure 2: The Propeller

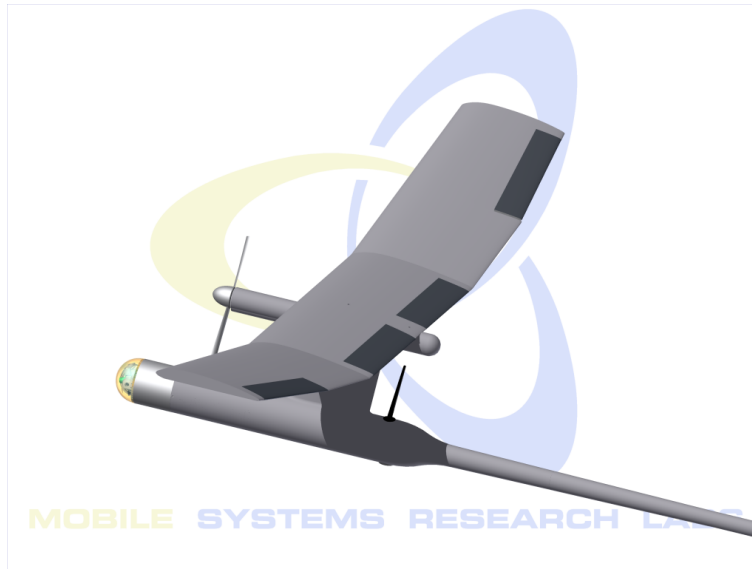


Figure 3: The Wing

### 2.1.2. The Wing

The wing is one of the most important parts of the plane, so the choice of the appropriate one for the Burzyk was crucial. The main criteria for choosing the airfoil were the lift force and maximal possible speed. Finally the trapezoidal wing with appropriate airfoil was chosen. Additionally a few tests according to wing dihedral were conducted. This operation allowed constructors to achieve even better stability of the flight and easy turning with use of ailerons. The wing has also the butterfly system installed, which enables very significant and fast but safe reduction of the altitude by special configuration of flaps and ailerons. The wingspan is 2.4m. The whole wing is assembled from 3 parts - two side and the central one. This is shown at picture 3

### 2.1.3. The Stabilizer

The horizontal stabilizer in the UAV is in the form of T-tail. Such a type of the stabilizer allows the plane to achieve very good lateral and longitudinal stability. Very important was proper size, that enables the plane to react correctly to the steering commands. Using such a type of horizontal stabilizer (all moving), one has to keep in mind that its maximal amount of throw is very little, but its effectiveness is large.

### 2.1.4. The Fuselage

One of the most important parts of the Burzyk is fuselage. It houses all electronic parts, engine and the batteries, that are responsible for powering the whole UAV's infrastructure. Fuselage consists of three main parts:

- Gimbal module
- Central part
- Tail part

The camera gimbal constitutes the front part of the fuselage which is directly attached to the central part. The central part is the biggest one. Its diameter is 100 mm in the cylindrical part. Here the most of the electronic modules are placed. They are responsible for the measurements and powering the whole UAV. The pylon, which enhances the lateral stability and enlarges the capacity, is placed in the upper part. Over the pylon the other cylindrical part of diameter 54 mm is placed. It houses the electrical engine. There is special aperture, designed for supplying

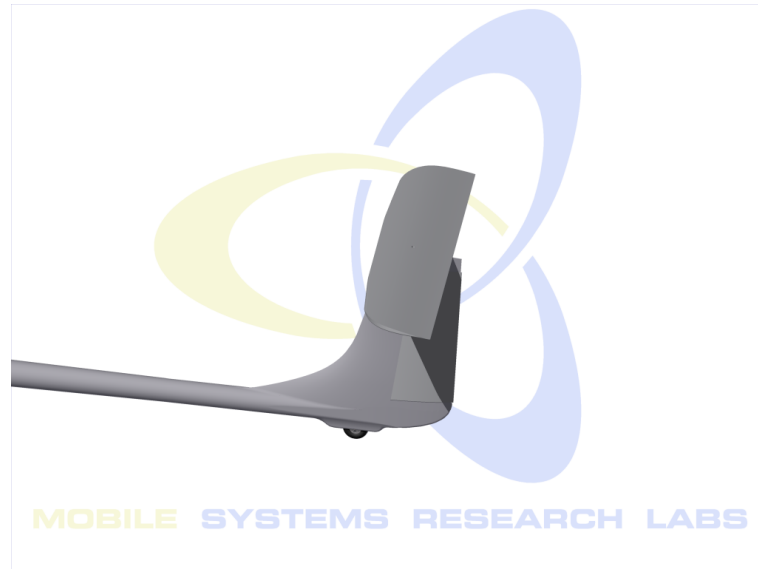


Figure 4: The Tail

air to cool the engine during the work. There is also rear part of the fuselage where the rudder and elevator are placed.

## 2.2. Launch systems

For the UAV to be operational Launch system is needed. Because ease of launch and applicability to different scenarios is very important for the end user different launch systems have been developed.

### 2.2.1. Wheels

Detachable wheeled launch system will be usable in most situations. It is shown in Figure 6.

For the UAV to launch 100m of closed road is needed. This system doesn't need any other maintenance.

### 2.2.2. Catapult

If there is no road available catapult launch system might be used. Catapult will be powered with compressed gas. This system is shown in Figure 7. Disadvantage of this system is that catapult must be recharged every 10-20 launches.

### 2.2.3. Hand

UAV can be launched from hand. It requires trained operator, and doesn't always succeed, but in crisis situation this launch method also might be used.

## 2.3. Summary

The Burzyk is lightweight UAV. Apart from the previously mentioned advantages there is one more: the operating costs. In comparison to real planes, Burzyk is amazing. Additionally it can be transported just by a single man. We can assume that assembling by one person takes approximately 10 minutes. The whole plane consists of 7 basic parts, these are: fuselage (3 parts), wing (3 parts), and the vertical stabilizer. Small size, easy assembling and applied technology, make Burzyk applicable in many branches of science and industry.

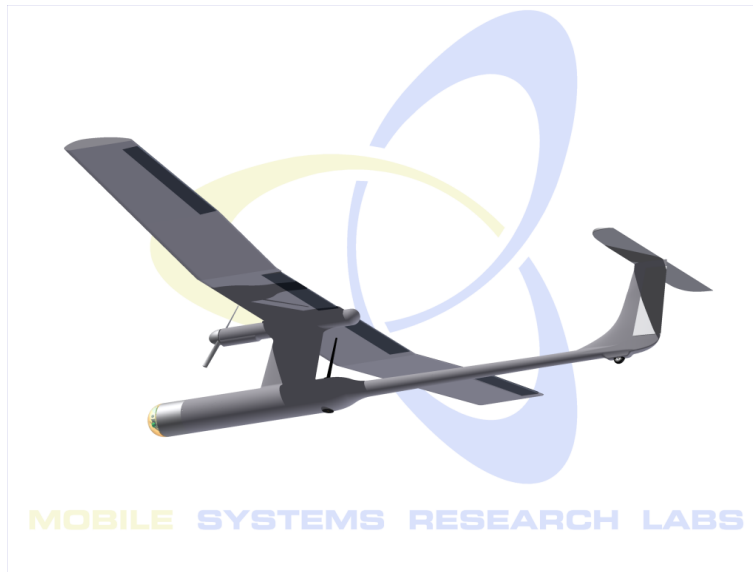


Figure 5: The Fuselage

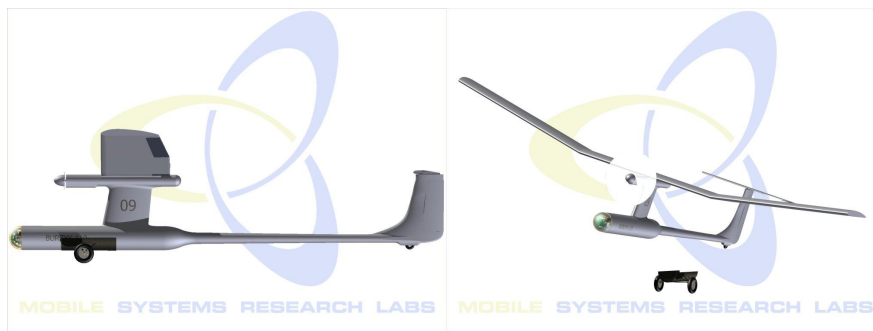


Figure 6: Wheeled launch

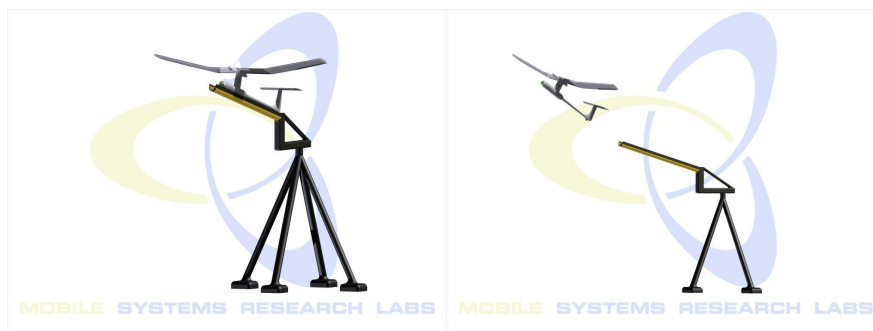


Figure 7: Catapult launch

## 3. Control

Autonomous control of an unmanned aircraft requires to design the control algorithms. This task can be accomplished in various ways, e.g. by designing proportional-integral-derivative (PID) controller, using modern nonlinear approaches or fuzzy algorithms. Control algorithms used in INDECT project must operate at low subsonic speeds, i.e. where Mach number is significantly lower than 1. Thus many effects occurring at high Mach numbers are not present. The design of control algorithms is simplified somehow and reduced to one of many cases.

Proper understanding of aircraft behavior during flight is necessary to design autonomous control. Thus in the following section a six-degree-of-freedom aircraft model is described. This allows to describe aircraft performance in Section 3.2 and control algorithms in Sections 3.3 and 3.4. Good reference on aircraft control is given in book [14] and notation used in this section is inspired mostly by this reference.

### 3.1. Equations of Motion

To describe aircraft's behavior formally a coordinate system and reference frame must be defined first. Aircraft tries to utilize aerodynamic forces that are acting on it because of presence in planet's atmosphere to counteract the effects of planet's gravity. Aircraft motion is strongly connected with the presence of planet which is assumed to be Earth.

The first frame of reference which is of interest for this document is Earth-centered inertial frame (ECI). Origin of this frame is placed at the Earth's center of mass. ECI frame is not rotating together with the Earth, this is an inertial frame and no external forces are present. The frame which has origin in Earth's center of mass and rotates with the Earth rotation is called Earth-centered, Earth-fixed (ECEF) frame. WGS84 coordinate system is defined in this frame together with WGS84 ellipsoid. At every point of this ellipsoid vector normal to the surface of ellipsoid forms an up vector. Vector orthogonal to the up vector which points to the direction of conventional terrestrial pole is called north vector. Third vector that completes right-handed coordinate system is called east vector. Those three vectors forms North-east-down (NED) coordinate system. This system is different for every point in Earth's frame. It will be used in particular along aircraft's flight path, defined for every position of aircraft's center of mass.

Frame of reference where equations of motion for aircraft's body are defined is called a body frame. It is frame rigid to vehicle's body with origin at vehicle's center of mass. Axes for this frame are defined with the help of vehicle's reference directions and consist a body-fixed coordinate system. X-axis is pointing to the aircraft's forward direction, y-axis is pointing to the right wing and z-axis is pointing in the aircraft's down. Two important aerodynamic angles are defined in body frame — angle-of-attack angle  $\alpha$  and side-slip angle  $\beta$ . The angle-of-attack angle is an angle spanned between xy plane and wind direction vector. Side-slip angle is an angle between xz plane and wind direction vector. Body-fixed coordinate system can be rotated around y-axis by special value of an angle of attack which is used in studying steady-state flight. This new coordinate system is a stability-axis coordinate system. This system can be rotated further around z-axis to match direction of the wind vector and form wind-axis coordinate system.

UAV considered in INDECT project is low-speed aircraft with limited range and capable of flying over rather small distances. Thus simplified equations of motion that do not take into account centripetal and Coriolis forces will be presented. Those forces are not significant for low-speed aircraft flying over small fragment of Earth.

Equations of motion will be defined in tangent-plane coordinate system at some location on Earth, e.g. this can be a location where UAV starts the flight. This system is a NED coordinate system and will be denoted by  $T$ . Position of an aircraft relative to  $T$  origin in  $T$  coordinate system is denoted by  $p$ . Velocity of an aircraft relative to this frame is denoted by  $v$  and is given in body coordinate system. Orientation of an aircraft (orientation of a body frame relative to tangent frame) is described by Tait-Bryan angles — yaw  $\psi$ , pitch  $\theta$  and roll  $\phi$ . Those angles are defined in different coordinate systems and do not form a vector. They are special form of Euler angles. Angles  $\psi$ ,  $\theta$ , and  $\phi$  will be identified by an array  $\Phi$ . For purposes of calculations

they are converted to matrix form (matrix of rotation) using conversion formulas:

$$C(\Phi) = \begin{bmatrix} \cos \theta \cos \psi & \cos \theta \sin \psi & -\sin \theta \\ (-\cos \phi \sin \psi + \sin \psi \sin \theta \cos \psi) & (\cos \phi \cos \psi + \sin \phi \sin \theta \sin \psi) & \sin \phi \cos \theta \\ (\sin \phi \sin \psi + \cos \psi \sin \theta \cos \psi) & (-\sin \phi \cos \psi + \cos \phi \sin \theta \sin \psi) & \cos \phi \cos \theta \end{bmatrix},$$

where  $C(\Phi)$  is rotation matrix that represents transformation from tangent plane to body frame. It will be denoted for short by  $C$ . Using transformation matrix  $C$ , the position (which is given in NED coordinate system) can be related to velocity (given in body coordinate system) using equation

$$\dot{p} = C^{-1}v. \quad (1)$$

Angular velocity of an aircraft's body frame relative to inertial frame (which is by assumption tangent-plane frame) is denoted by  $\omega$  and its components denoted as  $P$ ,  $Q$  and  $R$ ,

$$\omega = \begin{bmatrix} P \\ Q \\ R \end{bmatrix}.$$

Derivatives  $\dot{\psi}$ ,  $\dot{\theta}$  and  $\dot{\phi}$  are denoted by an array  $\dot{\Phi}$  and form the second state equation

$$\dot{\Phi} = H(\Phi)\omega, \quad (2)$$

where matrix  $H(\Phi)$  dependent on  $\Phi$  is given by

$$H(\Phi) = \begin{bmatrix} 1 & \tan \theta \sin \phi & \tan \theta \cos \phi \\ 0 & \cos \phi & -\sin \phi \\ 0 & \sin \phi / \cos \theta & \cos \phi / \cos \theta \end{bmatrix}.$$

The above equations relate position with its derivative and orientation angles with its derivatives. The third state equation describes effect of forces acting on an aircraft:

$$\dot{v} = \frac{F_{A,T}}{m} + Cg - \Omega(\omega)v, \quad (3)$$

where  $F_{A,T}$  is a sum of aerodynamic and thrust forces acting on the aircraft,  $m$  is an aircraft's mass and vector  $g$  is gravity vector. For purposes of flat-earth equation a simplified gravity model of the form  $g = [0, 0, g_D]$  can be used. The matrix  $\Omega(\omega)$  is a cross-product matrix of an angular velocity vector:

$$\Omega(\omega) = \begin{bmatrix} 0 & -R & Q \\ R & 0 & -P \\ -Q & P & 0 \end{bmatrix}.$$

The last equation required to describe aircraft's dynamic relates angular momentum  $M_{A,T}$  with angular velocity:

$$\dot{\omega} = J^{-1}(M_{A,T} - \Omega(\omega)J\omega), \quad (4)$$

and  $J$  is an inertia matrix:

$$J = \begin{bmatrix} J_{xx} & -J_{xy} & -J_{xz} \\ -J_{xy} & J_{yy} & -J_{yz} \\ -J_{xz} & -J_{yz} & J_{zz} \end{bmatrix}.$$

The inertia matrix elements are moments of inertia around x, y and z axes and cross-products of inertia. They are derived from mass distribution of an aircraft and describe its inertial behavior.

Equations 1, 2, 3 and 4 consists for complete aerodynamics model that describes aircraft's motion in flat-Earth model. Aircraft's state vector is composed of quantities mentioned above (position  $p$ , orientation  $\Psi$ , velocity  $v$ , angular velocity  $\omega$ ) and is denoted by  $X$ :

$$X = \begin{bmatrix} p \\ \Phi \\ v \\ \omega \end{bmatrix}.$$

Given the initial state  $X_0$ , forces acting on an aircraft  $F_{A,T}$ , moments acting on an aircraft  $M_{A,T}$  and its mass properties (mass  $m$  and inertia matrix  $J$ ) the equations of motion can be solved and aircraft's behavior studied.

For studying aerodynamics effects an important quantity is aircraft's velocity relative to wind mass. If  $v_W$  is wind velocity vector given in tangent-plane coordinate system then relative velocity  $v_{rel}$  is described by formula

$$v_{rel} = v - Cv_w.$$

The vector negative to  $v_{rel}$  is called a relative wind. Magnitude of the wind velocity vector  $v_w$  is denoted by  $V_T$ , a free-stream airspeed.

### 3.2. System Identification

An aircraft is able to fly and sustain itself in the air because of the forces acting on it. There are two sources of forces that are important when analyzing flying qualities — aerodynamic force and thrust force. The source of thrust force is an engine and in INDECT project only electric propeller engines are considered. The main purpose of thrust is to gain velocity and velocity relative to wind is one of the main factors for appearance of aerodynamic force. Three components of the aerodynamic force are: drag  $D$  which is acting in negative direction of x-axis in body frame (to the aircraft's back), lift  $L$  which is acting in negative direction of z-axis in body frame (to the aircraft's up) and crosswind force  $C$  which is acting in negative direction of y-axis in body frame (to the aircraft's left). Beside aerodynamic force  $F_A$  an important quantity is an aerodynamic moment  $M_A$  and its x, y and z components are accordingly rolling moment  $l$ , pitching moment  $m$  and yawing moment  $n$ .

Aerodynamic forces and moments are caused by the presence of every aircraft fragment — fuselage, wings, rudder, elevator and other elements like landing gear. The main purpose of wing is to create a lift force and as a result a significant drag force is also created. Cross-section of a wing is called an airfoil. Because of curved shape the air around an airfoil does not pass with an equal speed. The pressure difference between upper and lower surfaces of an airfoil is non-zero. This results in non-zero lift force. Lift force is dependent on the angle-of-attack  $\alpha$ , i.e. different alignment of the wing relative to wind velocity vector results in change of lift and drag components. With varying  $\alpha$  a significant change in pitching moment also occurs.

Similar analysis can be performed for other elements of an UAV and can be found in literature on aircraft aerodynamics. To describe overall behavior of an aircraft a collection of aerodynamic coefficients is constructed. The effect of the surrounding air on forces and moments is varying with air conditions. This influence is proportional to dynamic pressure  $\bar{q}$  which is proportional to the air density  $\rho$  and airspeed  $V_T$ :

$$\bar{q} = \frac{1}{2}\rho V_T.$$

Dynamic pressure is used to formulate forces and moments formulas. Aerodynamic coefficients are dependent on the aircraft properties (geometry, boundary material) and the surrounding fluid (which is an Earth's atmosphere in this case) — its viscosity  $\mu$ , which describes fluid's resistance to the rate of change of shape and density  $\rho$ , which denotes to what extent the fluid is compressed. Geometrically similar airfoils (the same shape, the same definition of reference but not necessarily the same size) have equal aerodynamic coefficients provided that two special parameters — similarity parameters are the same. The first similarity parameter is a Reynolds number  $R_e$  which combines fluid properties and aircraft's characteristic length  $l$ :

$$R_e = \frac{\rho l V_T}{\mu}.$$

For an aircraft the characteristic length is usually mean chord of the wing. The second similarity parameter is a free-stream Mach number  $M$ :

$$M = \frac{V_T}{a},$$

and  $a$  is the speed of sound in considered fluid. When both  $R_e$  and  $M$  are equal then an airfoil will have the same aerodynamic coefficient for geometrically similar airfoils (in particular of

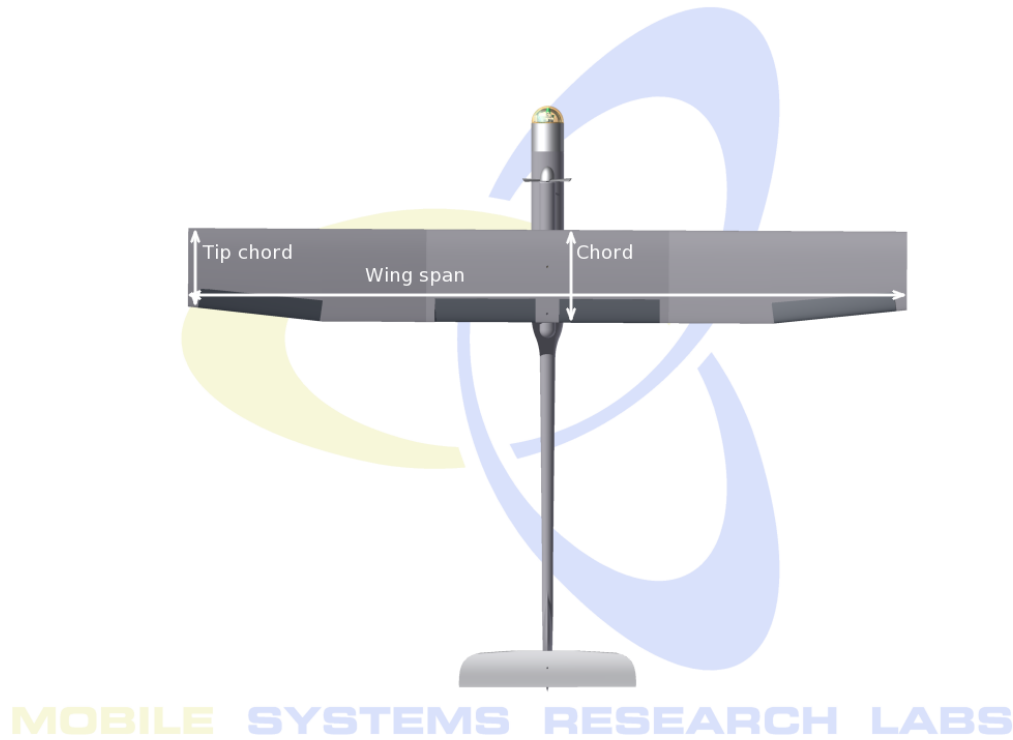


Figure 8: Geometrical characteristics of a wing.

different size airfoils). Thus for an airfoil the aerodynamic coefficient  $C$  is a function of  $\alpha$ ,  $M$  and  $R_e$  —  $C(\alpha, M, R_e)$ . For an aircraft there are three general dimensionless force coefficients denoted by  $C_D$ ,  $C_L$ ,  $C_C$  and three dimensionless moments coefficients denoted by  $C_l$ ,  $C_m$ ,  $C_n$ . They are however dependent on additional system parameters — side-slip angle  $\beta$ , rudder, elevator or ailerons deflection and  $\alpha$ ,  $\beta$  derivatives. Relation between forces, moments and aerodynamic coefficients is given by set of equations:

$$\begin{aligned} D &= \bar{q} S C_D \\ L &= \bar{q} S C_L \\ C &= \bar{q} S C_C \\ l &= \bar{q} S b C_l \\ m &= \bar{q} S \bar{c} C_m \\ n &= \bar{q} S b C_n \end{aligned}$$

Coefficients  $S$ ,  $b$  and  $\bar{c}$  are aircraft's geometrical parameters —  $S$  is a total wing area,  $b$  is wing span and  $\bar{c}$  is a mean aerodynamic chord ( $c$  is a wing chord). The total wing area is a sum of the area of lower and upper wing surface. Figure 8 shows the geometrical representation of the wing span and the wing chord parameters. Chord is not constant across the wing and because of that in force equation a different parameter is used — mean aerodynamic chord. Mean aerodynamic chord is constant for given aircraft and denotes a width of an equivalent rectangular wing in given conditions. Aerodynamic coefficients are usually decomposed to independent quantities e.g. drag coefficient is decomposed to parasite drag, induced drag and wing drag. Detailed analysis can be found in textbooks on aircraft aerodynamics.

With this set of equations the aerodynamic forces and moments can be obtained. Together with thrust forces and moments they can be used to provide force  $F_{A,T}$  and moment  $M_{A,T}$  for state equations 1, 2, 3 and 4. Aircraft flight can now be simulated or studied algebraically. For controlling the aircraft an important issue is a static analysis. Small perturbations from steady-state conditions are analyzed. Aircraft's stability and performance can be evaluated.

The first step required to perform a static analysis is a linearization of aircraft's state equation. This procedure requires the computation of state functions gradients and produces a number of derivatives called stability derivatives which are dependent on aerodynamic coefficients. Linearization procedure can be performed in specific conditions which puts the aircraft system in an equilibrium point (also singularity point). The conditions are dependent on flight conditions. For every case of steady-state flight conditions the angular rate derivatives  $\dot{P}$ ,  $\dot{Q}$ ,  $\dot{R}$  and airstream velocity derivatives  $\dot{V}_T$ ,  $\dot{\alpha}$ ,  $\dot{\beta}$  are set to 0. Other parameters are different for various maneuvers, e. g.:

**Wings-level flight:** Roll  $\phi$  is set to 0 and angular velocity is set to 0:  $\dot{\phi}, \dot{\theta}, \dot{\psi} \equiv 0$ .

**Turning flight:** Yaw rate  $\dot{\psi}$  is set to constant value, other rates are set to zero:  $\dot{\phi}, \dot{\theta} \equiv 0$ .

**Pull-up:** Pitch rate  $\dot{\theta}$  is set to constant value, other rates and roll are set to zero:  $\dot{\phi}, \dot{\psi} \equiv 0$ .

**Roll:** Roll rate  $\dot{\phi}$  is set to constant value, other rates are set to zero:  $\dot{\theta}, \dot{\psi} \equiv 0$ .

With the state equation linearized near this flight conditions various transfer functions of an aircraft can be evaluated and controller for the designed system.

For some purposes (e.g. simulation or advanced controller design) this simplified, linear model of an aircraft's dynamics is not sufficient. The nonlinear aircraft's model is then used. In this case algebraical manipulations are usually too complicated and only numerical methods are applicable.

### 3.3. Control Algorithms Overview

Classical control theory is being developed since the beginning of flight. There were always a need to relief and support human pilot in piloting the aircraft. Nowadays some types of planes are designed to be unstable in order to improve flying qualities. In planes like this stability augmentation systems and control augmentation systems are not only addition but necessity. Similarly, for the unmanned air-crafts an autonomous flight is very often a necessary feature.

Development of autopilots is historically influenced by human factors in a great level. Large part of autopilot development is dedicated to analysis of handling qualities. Those handling qualities are summarized in pilot opinion rating scales, e.g. Cooper-Harper scale. However, those qualities are not applicable to unmanned aircraft used in INDECT project because no human presence is involved.

The design of classical autopilot involves detailed analysis of aircraft transfer functions near the aircraft's stability conditions. They are obtained from stability derivatives. Some handling qualities dictating autopilot design places constraints on poles and zeros of aircraft transfer functions. Appropriate regulators are designed to control pitch, roll, yaw and speed of the aircraft with desired constraints.

With the development of digital computers an alternative approaches to aircraft's control became possible. Modern techniques rely less on the engineering judgment and introduce quantitative quality estimations. Quality is now described by performance criterion. It is desirable to select a time-domain quality index and one of them is quadratic performance index of the form

$$J = \frac{1}{2} \int_0^{\infty} (x^T Q x + u^T R u) dt,$$

where  $Q$  and  $R$  are positive semi-definite weighting matrices,  $x$  are state variables and  $u$  are control variables. The goal of controller design is to minimize the performance index. This approach is used in linear quadratic regulator. When applied to regulator with many closed-loops this technique can be used to determine all control gains simultaneously. Various techniques for determining the actual form of performance index or determining gains are developed including power-full model-following design.

However, aircraft responses and flight dynamics is highly nonlinear. Linear control derived from classical control theory approximates this behavior only in specific conditions. There are modern nonlinear approaches to aircraft's control like dynamic inversion design. To implement this technique a complete aircraft's dynamic model must be known. Control outputs are solved simultaneously to follow desired reference trajectory using aircraft state equations obtained

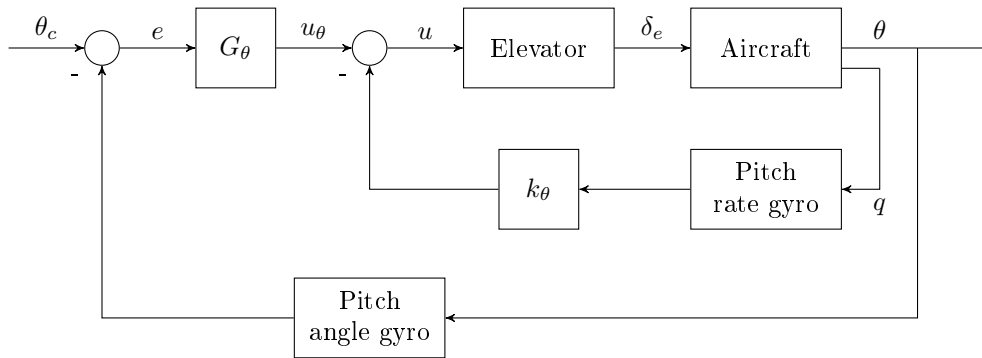


Figure 9: Pitch-attitude hold controller overview.

from aircraft model. Using this approach the main advantage over classical controller is that it can work in every flying conditions, e.g. in high angle-of-attack or in a wide range of velocities. However, implementation of such design is quite complex task.

### 3.4. PID Controllers

Classical control theory is a common tool during aircraft’s autopilot design. Poles and zeros of UAV’s transfer functions are analyzed around steady-state flight conditions. Steady-state flight conditions allows for linearization of aircraft’s flight dynamics. Appropriate regulators and dynamic compensators are designed with the knowledge of those transfer functions and desired aircraft behavior can be obtained.

Because of that smaller autopilot components have a small range of application and they must be controlled by higher-level mechanism which takes into account operational ranges of specific regulators. Besides those disadvantages the classical control is power-full and can form a complete autopilot system.

#### 3.4.1. Pitch Hold

Pitch attitude hold controller is designed to hold pitch angle  $\theta$  equal to the reference control value  $\theta_c$ . The flight-path angle  $\gamma$  that spans between aircraft’s velocity vector and north-east plane is not held constant, thus in practice this controller is not used directly. Pitch attitude hold controller is used as a fragment of altitude hold or automatic landing controllers. An overview of pitch attitude hold controller is presented in Figure 9. Error  $e$  between current pitch angle and desired pitch angle is forwarded to pitch angle dynamic compensator  $G_\theta$ . Output  $u_\theta$  of this compensator can be compared with pitch angle rate  $q$ , as presented on the diagram. The goal of this inner-loop is to improve short-period regulatory behavior. Constant  $k_q$  provides flexibility for accounting short-period effects. The final control signal  $u$  regulates the elevator servo and changes elevator deflection angle  $\delta_e$ .

Dynamic compensator component  $G_\theta$  is designed using P, I and D regulators. Regulators and appropriate parameters are chosen based on analysis of flight history or simulated and estimated aircraft behavior. They are different for various UAVs and are chosen separately for each of them.

#### 3.4.2. Altitude Hold

Altitude hold is designed to regulate aircraft’s altitude at reference value  $h_c$ . Reference altitude is obtained from GPS or atmospheric pressure measurements (barometer measurements). When using barometer measurements a time lag must be included. Altitude measurement obtained from this sensor are delayed.

Altitude regulator uses pitch hold regulator to control pitch rate and make altitude corrections. Dynamic compensator used by altitude regulator is controlled by an altitude error and regulates pitch angle. It is often desired for an altitude dynamic compensator to have relatively

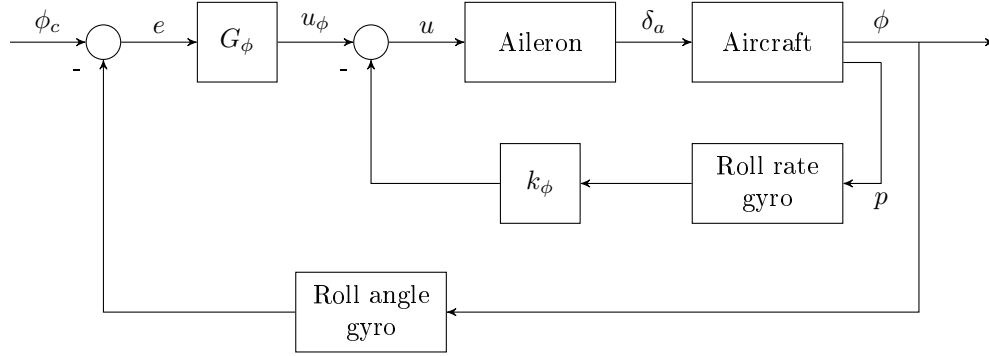


Figure 10: Roll-attitude hold controller overview.

slow response and reject low frequency disturbances. Lead-lag compensation is commonly used in altitude control.

### 3.4.3. Roll Hold

Roll angle regulator is used to control wings-level angle or angle different than wings-level during the turns. Its design is similar to the pitch hold autopilot and is presented in Figure 10. Reference angle  $\phi_c$  is used to regulate roll angle  $\phi$ . Error between roll angle  $\phi$  and reference angle  $\phi_c$  is forwarded to dynamic compensator  $G_\phi$ . Inner loop with gain from roll rate gyro is used to compensate for short period oscillations of roll angle. Output  $u$  regulates the ailerons angle deflection  $\delta_a$ .

When roll angle is set to value other than wings-level flight then pitch and yaw angles are affected and they are changing. Roll hold autopilot is together with pitch hold autopilot necessary component needed to make a coordinated turn of the UAV.

### 3.4.4. Coordinated Turn

The perfect coordinated turn is a turn where force component along aircraft's Y axis in body frame is equal to zero. This turn has advantage for passenger air-crafts and gives them flying comfort. Coordinated turn is characterized by high aerodynamic efficiency and minimized load on the aircraft structures. Those factors are also important for UAVs. Coordinated turn can be crucial for aircraft mission like video surveillance or transport and correlated with them.

During coordinated turn roll angle rate  $\dot{\phi}$  and pitch angle rate  $\dot{\theta}$  are set to zero and yaw angle rate  $\dot{\psi}$  is set to desired turn rate value. An approximate dependency between roll, pitch and yaw angles during coordinated turn for steady-state flight conditions is given by

$$\tan \phi = \frac{\dot{\psi}}{g_D} \frac{V_T}{\cos \theta}.$$

One can set pitch angle to be held constant at  $\theta \approx 0$ , thus  $\cos \theta \approx 1$ . In this case roll angle is obtained from the above equation for specific turn rate  $\dot{\psi}$ . However, this is not a rule and the value for pitch angle can also vary (with appropriately varying roll angle) and appropriate altitude of an UAV can be regulated during coordinated turn. Coordinated turn uses pitch angle regulator together with roll angle regulator to perform the turn.

### 3.4.5. Heading Hold

Heading hold autopilot regulates coordinated turn autopilot. It compares reference heading value with the true heading obtained from GPS measurements or magnetic heading obtained from compass measurements. It calculates appropriate yaw angle rate  $\dot{\psi}$  for coordinated turn autopilot. Together with altitude hold autopilot it forms a basic but complete autopilot that can be used during the flight.

### 3.4.6. Automatic Landing

Automatic landing system is composed of two phases — the approach phase and the flare control phase. During the approach phase aircraft's altitude and speed are regulated by the altitude autopilot and thrust regulator.

During the approach phase aircraft trajectory must follow an imaginary straight line that is directed upward from the ground at small angle and in parallel to the landing place. This line is called a glide path and any deviations from this path are compensated using pitch and heading angles autopilots. During the approach phase the airspeed must be low. However, it must not drop below specific threshold value (for given aircraft) where UAV would stall and loose maneuverability.

At approximately 15m above the ground the approach phase ends and flare control takes place. During this phase the aircraft's rate of descent and airspeed are reduced. The pitch angle is set to value appropriate for landing, it is rapidly increased to the value of a few degrees. Also the engine thrust is reduced. A few seconds later UAV lands.

## 4. Localization

### 4.1. Overview

For precise localization a number of sources must be used and then data from them must be combined together with filtering.

### 4.2. GPS

The Global Positioning System (GPS) is a Global Navigation Satellite System (GNSS) which provides continuous, world-wide three-dimensional position and velocity information to users with appropriate receiving equipment. The system is comprised of three functional segments:

- The space segment nominally consisting of 24 satellites is arranged in 6 orbital planes with 4 satellites per plane orbiting the Earth at a height of 20,180km. As of May 2010 there are currently 29 satellites in orbit and healthy. It is due to their pattern of distribution and to the high orbital altitudes that communication with at least 4 satellites is ensured at all times anywhere in the world.
- The control segment which consists of a Master Control Station in the state of Colorado, five monitoring stations and three ground control stations transmitting information to the satellites. This segment performs various tasks including: observing the movement of the satellites and computing current orbital data (ephemeris), monitoring and synchronizing the onboard satellite time, relaying information such as satellite health, clock errors, etc.
- The user segment: civilian and military users equipped with GPS receivers.

The system utilizes the concept of one-way Time of Arrival (TOA) ranging. Satellite transmissions are referenced to highly accurate atomic frequency standards onboard the satellite, which are synchronised with a GPS time base. The satellites broadcast ranging codes and navigation data on two frequencies using a technique called code division multiple access (CDMA); that is, there are only two frequencies in use by the system, L1 (1,575.42 MHz) and L2 (1,227.6 MHz). Each satellite transmits on these frequencies, but with different ranging codes than those employed by other satellites. These codes were selected because they have low cross-correlation properties with respect to one another. Each satellite generates a short code referred to as the Coarse/Acquisition code (C/A) and a long code denoted as the precision or P(Y) code (encrypted, for military use). The navigation data provides the means for the receiver to determine the location of the satellite at the time of signal transmission, whereas the ranging code enables the user's receiver to determine the transit time of the signal and thereby determine the satellite-to-user range. This technique requires that the user receiver also contain a clock. Utilizing this technique to measure the receiver's three-dimensional location requires that TOA ranging measurements be made to four satellites. If the receiver clock were synchronized with the satellite clock, only three range measurements would be required. However, a crystal clock

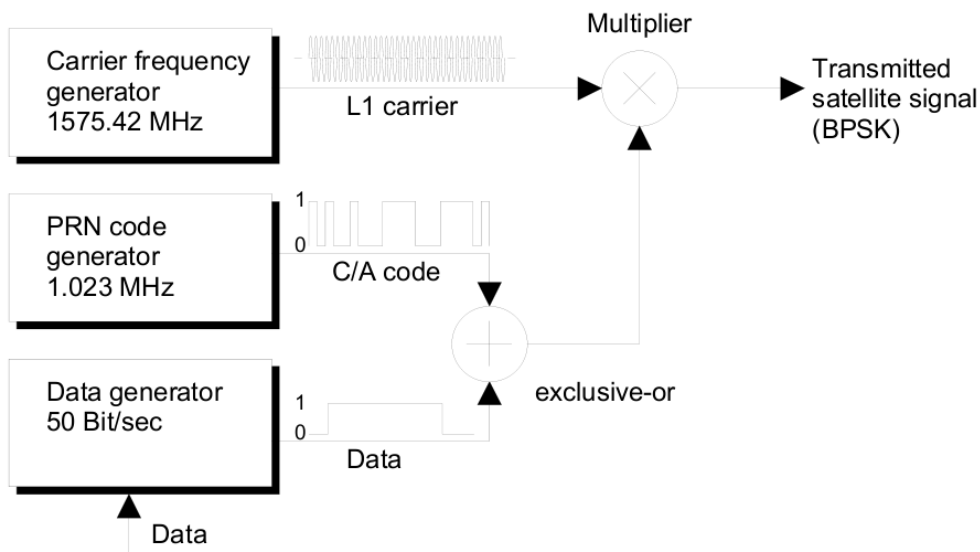


Figure 11: GPS signal modulation

is usually employed in the navigation receivers to minimize the cost, complexity, and size of the receiver. Thus, four measurements are required to determine user latitude, longitude, height and receiver clock offset from internal system time. If either system time or height is accurately known, less than four satellites are required [6].

#### 4.2.1. Principles of Operation

GPS satellites are equipped with four highly accurate atomic clocks. The resonance frequency of one of these clocks is used to generate the following signals:

- the frequency of the carrier signal - L1 for civil and L2 for military use.
- the 50 Hz data pulse which carries the Navigation Message (GPS time, coarse and precise satellite orbital data - almanac and ephemeris).
- the C/A code which modulates the data using the exclusive-or operation spreading the data over a 2 MHz bandwidth. This process is known as Direct Sequence Spread Spectrum (DSSS) modulation which deliberately spreads a nominal signal over a wider bandwidth making it less prone to narrowband interference. The use of Pseudo Random Noise (PRN) code which is different for each satellite enables concurrent transmission from all the satellites on the same frequency. This is called Code Division Multiple Access (CDMA) multiplexation.

The data modulated by the C/A code modulates the L1 carrier in turn by using Binary Phase Shift Keying (BPSK). The process is shown in Figure 11.

In order for the receiver to determine its position, it must receive time signals from four separate satellites in order to calculate the signal travel times  $\Delta t_1 \dots \Delta t_4$ . Calculations are effected in Cartesian, three-dimensional coordinate system with a geocentric origin (Figure 12). The range of the four satellites  $R_1, R_2, R_3, R_4$  can be determined with the help of signal travel times  $\Delta t_1, \Delta t_2, \Delta t_3, \Delta t_4$  between the four satellites and the user. As the locations  $X_{sat}, Y_{sat}, Z_{sat}$  of the four satellites are known (from almanac and ephemeris), the user coordinates can be calculated.

Due to the atomic clocks onboard the satellites, the time at which the satellite signal is transmitted is known very precisely. All satellite clocks are adjusted or synchronized with each other and UTC (Universal Time Coordinated). In contrast, the receiver clock is not synchronized to UTC and is therefore slow or fast by  $\Delta t_0$ . The time error causes inaccuracies in the measurement of signal travel time and the distance  $R$ . As a result, an inaccurate distance

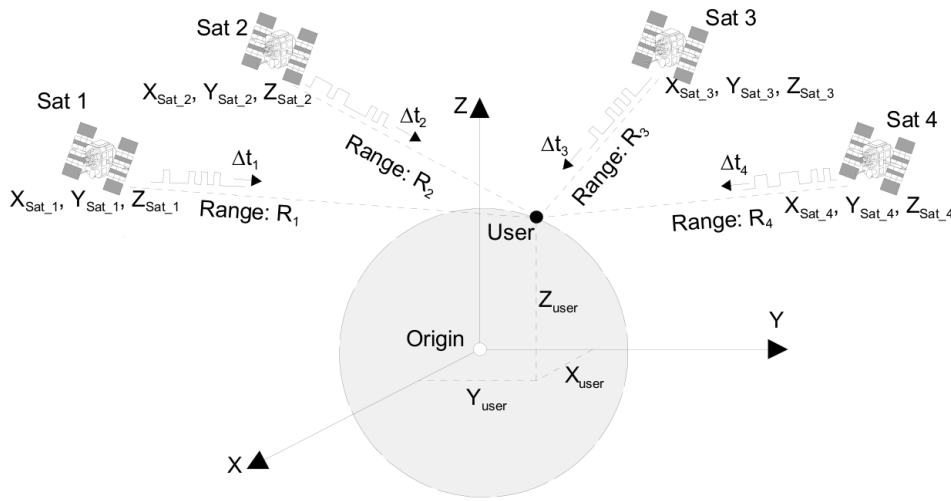


Figure 12: Coordinate system

is measured that is known as pseudo distance or pseudorange  $PSR$ .

$$\begin{aligned}\Delta t_{measured} &= \Delta t + \Delta t_0 \\ PSR &= c\Delta t_{measured} = c(\Delta t + \Delta t_0) \\ PSR &= R + c\Delta t_0\end{aligned}$$

where  $R$  is true range of the satellite from the user,  $c$  is the speed of light,  $\Delta t$  is the signal travel time from the satellite to the user,  $\Delta t_0$  is the difference between the satellite clock and the user clock and  $PSR$  is the pseudorange.

In order to determine the four unknown variables ( $\Delta t_0, X_{user}, Y_{user}, Z_{user}$ ) four independent equations are necessary. The following is valid for the four satellites ( $i = 1 \dots 4$ ):

$$PSR_i = \sqrt{(X_{sat_i} - X_{user})^2 + (Y_{sat_i} - Y_{user})^2 + (Z_{sat_i} - Z_{user})^2} + c\Delta t_0$$

The equations are linearized and solved in a few iterations until errors components are smaller than the desired error [16].

#### 4.2.2. Performance of Stand-Alone GPS

The accuracy with which a user receiver can determine its position or velocity, or synchronize to GPS system time, depends on a complicated interaction of various factors. The precision of positioning with GPS navigation depends on one hand on the precision of the individual pseudorange measurements and on the other hand on the geometric configuration of the satellites used. Determination of position is more difficult if the four reference satellites being used for measurement are close together. This configuration is expressed in terms of a scalar value, which is referred to in navigation literature as DOP (Dilution of Precision). The pseudorange measurements are influenced by [6, 16]:

- Satellite clock error: even though the satellite onboard atomic clocks are highly stable, the clock correction fields in the navigation data message are sized such that the deviation between satellite time and GPS time may be as large as 1 ms which translates to a 300 km pseudorange error. The control center determines and transmits clock correction parameters to the satellites for rebroadcast in the navigation message. It is expected that residual clock errors will continue to decrease as newer satellites are launched with better performing clocks and as improvements are made to the control segment. Average clock errors are also influenced by the frequency of uploads to each satellite.
- Ephemeris error: estimates of ephemerides for all satellites are computed and uplinked to the satellites with other navigation data message parameters for rebroadcast to the user. The residual satellite position error is of range 1-6 m.

Error cause and type	Error without DGPS/SBAS	Error with DGPS/SBAS
Ephemeris data	1.5 m	0.1 m
Satellite clocks	1.5 m	0.1 m
Effect of the ionosphere	3.0 m	0.2 m
Effect of the troposphere	0.7 m	0.2 m
Multipath reception	1.0 m	1.4 m
Effect of the receiver	0.5 m	0.5 m
Total RMS value	4.0 m	1.2 m
Horizontal error (1-Sigma (68%) HDOP=1.3)	6.0 m	1.8 m
Horizontal error (2-Sigma (95%) HDOP=1.3)	12.0 m	3.6 m

Table 1: Achievable positioning accuracy

- Speed of light: the signals from the satellite travel at the speed of light. These slow down when crossing the ionosphere and troposphere and cannot be assumed to be a constant. This deviation from the normal speed of light creates error in the calculated position.
- Multipath: the error is caused by reception of reflected signals.
- Signal travel time error measurements: the GNSS receiver is only able to determine the time of the incoming satellite signal with limited accuracy.

The achievable positioning accuracy is presented in Table 1 along with possible improvements made by augmentation systems.

### 4.2.3. Augmentations

DGPS + SBASS (especially useful in aviation) and their performance are presented in Table 1.

## 4.3. IMU

### 4.3.1. Overview

Inertial navigation system is a navigation aid that uses motion and rotation sensors (accelerometers and gyroscopes) to calculate the position, orientation and velocity of UAV without the need for external references. IMU - Inertial measurement unit is a sensor containing all required components. In this section 6 degrees of freedom sensor will be described.

The main advantages of this system are:

- high measurement frequency - (systems with frequency of 300Hz are common)
- independence from external factors.

Disadvantages:

- Accumulated error

INS is used in short periods of time between measurements of other systems which don't suffer from accumulated error, but have smaller frequency.

### 4.3.2. Accelerometers

Accelerometer is a sensor of acceleration. Usually in 6DOF IMU 3 accelerometers are used - each for single axis. Generally accelerometer is a known mass on a spring. When sensor experiences acceleration, displacement is measured to calculate acceleration.

Currently most common technology is MEMS (micro electro-mechanical systems) which incorporates rule described above in micro-scale. Another popular technology is based on piezoresistors measuring spring tension.

	GG1320AN (Laser Gyro)	GG5300 (MEMS 3xGyro)
Size	88 mm×88 mm×45 mm	50 mm×50 mm×30 mm
Weight	454 g	136 g
Start-Up Time	< 4 s	< 1 s
Power	5 Vdc, 0.375 W nominal	5 Vdc, < 4 W
Operating Temperature Range	-54 °C to 85 °C	-45 °C to 85 °C
Bias Stability	0.0035 °/h	< 70°/h
Angular Random Walk	0.0035 °/√h	0.2 °/√h

Figure 13: Gyroscope systems comparison [1, 2]

### 4.3.3. Gyroscopes

Gyroscope is a device for measuring orientation. Most modern gyroscopes are measuring angular speed which has to be integrated in order to maintain orientation.

**Mechanical** A mechanical gyroscope is essentially a spinning wheel or disk whose axle is free to take any orientation. This orientation changes much less in response to a given external torque than it would without the large angular momentum associated with the gyroscope’s high rate of spin. Since external torque is minimized by mounting the device in gimbals, its orientation remains nearly fixed, regardless of any motion of the platform on which it is mounted. [15]

**Vibration** the basic principle of operation of such sensors is that the vibratory motion of part of the instrument creates an oscillatory linear velocity. If the sensor is rotated about an axis orthogonal to this velocity, a Coriolis acceleration is induced. This acceleration modifies the motion of the vibrating element and provided that this can be detected, it will indicate the magnitude of the applied rotation.[15]

**MEMS** gyroscopes are non-rotating devices and use the Coriolis acceleration effect on a vibrating proof mass(es) to detect inertial angular rotation. Thus, these sensors rely on the detection of the force acting on a mass that is subject to linear vibratory motion in a frame of reference which is rotating about an axis perpendicular to the axis of linear motion. The resulting force, the Coriolis force, acts in a direction, that is perpendicular to both the axis of vibration and the axis about which the rotation is applied. Whilst there are many practical sensor configurations based upon this principle.[15]

**Optical** gyroscopes use an interferometer or interferometric methods to sense angular motion. In effect, it is possible to consider the electromagnetic radiation as the inertial element of these sensors. In optical sensor light beam is projected in the same direction as sensed rotation axis (it is directed by mirrors or fiber). Rotation speed is measured as a difference in frequency, because light speed is constant.[15]

### 4.3.4. Inclinator

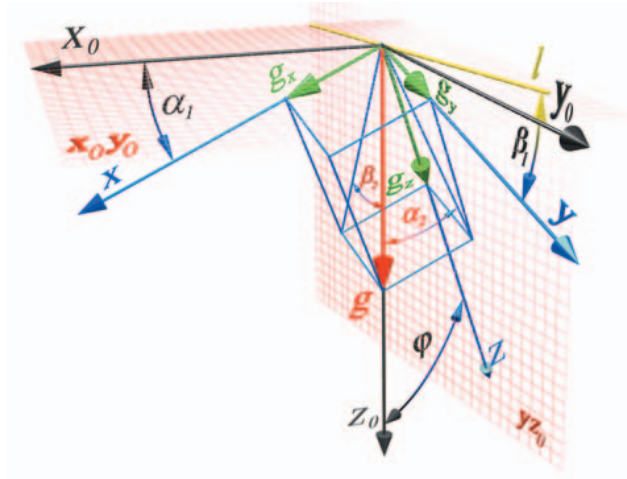
Inclinometer is a device which measures orientation basing on earth gravity acceleration. Principle of this device is that when there are no other accelerations than gravity the orientation of UAV can be calculated (Figure 14) (in roll and pitch axis).

The biggest problem with inclinometer is assumption, that there are no other accelerations than gravity. In practical situations error can be calculated

## 4.4. Magnetic sensors

### 4.4.1. Overview

Magnetic sensors measure magnetic field surrounding UAV. Assuming that there are no other magnetic fields a 3D sensor can measure bearing to Earth’s magnetic field. There are known errors of this measurement (deviation and declination), and appropriate correction methods are known.



$$\begin{aligned}\alpha_1 &= \arcsin \frac{g_x}{g} \\ \beta_1 &= \arcsin \frac{g_y}{g} \\ \alpha_2 &= \arctan \frac{\frac{g_x}{g}}{\sqrt{\frac{g_y^2}{g^2} + \frac{g_z^2}{g^2}}} \\ \beta_2 &= \arctan \frac{\frac{g_y}{g}}{\sqrt{\frac{g_x^2}{g^2} + \frac{g_z^2}{g^2}}}\end{aligned}$$

Figure 14: Inclinometer [8]

However often there are sources of magnetic field (power lines, buildings, radio transmitters), which add noise to the measure.

#### 4.4.2. Errors and performance

**Deviation** is an error created by UAV's own magnetic field. This error is different with different bearings and with different operational subsystems. Method of correction of this error is based on measuring this error and creating a correction table.

**Declination** is a difference between Earth's magnetic north and geographical true north. This difference is different in different places. There are agencies responsible for measuring magnetic field and publishing correction for navigation need [10].

**Random** magnetic field generated by other objects is the error, which cannot be compensated. There is a possibility to measure this error. Earth field intensity maps are also published[11], so it is possible to measure the difference between natural magnetic field and random magnetic field, and to calculate measurement error.

### 4.5. Aerometric sensors

#### 4.5.1. Overview

Aerometric sensor measures air flow surrounding UAV. There are 4 kinds of sensors:

**Static** sensor measures static pressure surrounding vehicle. With this sensor UAV height can be determined from barometric formula and standard atmosphere model.

**Vertical speed indicator** measures vertical speed based on difference between static measures.

**Dynamic** sensor measures dynamic pressure of air flow. With this sensor UAV speed can be calculated. This sensor needs a Pitot tube.

**Angular sensors** (angle of attack and sideslip angle) are sensors, which allow to calculate angle between airflow and UAV. This is important for calculating drag, lift and other basic aerodynamic forces acting on airplane surfaces.

#### 4.5.2. Errors and performance

**Static and VSI** sensors are very error prone, because they use complex atmosphere model for calculation. Often real atmosphere acts locally different than the model. Other problem is related to ground pressure - static sensor calculates height compared to ground pressure, if ground measurement is inaccurate then height measurement is also inaccurate. However in good conditions this sensor has accuracy of 5m. It isn't much if a UAV is close to ground, but it's enough when flying higher.

**Dynamic and angular** sensors are very accurate, because they measure air flow surrounding UAV, and all data needed for calculation is measured by aerometric sensors. These sensors have accuracy of 1 Mph or 1°.

### 4.6. Filtering

#### 4.6.1. Kalman Filter overview

Kalman filter and its extensions are the most popular methods of statically optimal estimation.

Using this tool it is possible to find value of unmeasurable variables with data from measurable variables and mathematical model which is connecting both types of variables.

Some Kalman filter (KF) properties[9]:

- KF is a optimal estimator, because under certain conditions it can minimize some criteria e.g. average square error of estimated parameters.
- Other fact proving optimal character of KF is that it uses all measures, no matter how big is their error. All measurements improve state estimation.
- KF is a recursive algorithm

#### 4.6.2. The discrete-time Kalman filter algorithm

This is a summary of discrete-time Kalman filter algorithm[13].

1. Dynamic state is given by the following equations:

$$x_k = F_{k-1}x_{k-1} + G_{k-1}u_{k-1} + w_{k-1}$$

$$y_k = H_k x_k + v_k$$

$$E(w_k w_j^T) = Q_k \delta_{k-j}$$

$$E(w_k v_j^T) = R_k \delta_{k-j}$$

$$E(w_k v_j^T) = 0$$

Where:

- $E(x)$  is mean value of  $x$
- $u_k$  is known input and  $w_k$  is white noise with covariance  $Q_k$ .

2. Kalman filter is initialized as follows:

$$\hat{x}_0^+ = E(x_0)$$

$$P_0^+ = E[(x_0 - \hat{x}_0^+)(x_0 - \hat{x}_0^+)^T]$$

3. Kalman filter is given by the following equations, which are computed for each step  $k = 1, 2, \dots$ :

$$P_k^- = F_{k-1} P_{k-1}^+ F_{k-1}^T + Q_{k-1}$$

$$\begin{aligned} K_k &= P_k^- H_k^T (H_k P_k^- H_k^T + R_k)^{-1} \\ &= P_k^+ H_k^T R_k^{-1} \end{aligned}$$

$$\hat{x}_k^- = F_{k-1} \hat{x}_{k-1}^+ + G_{k-1} u_{k-1} =$$

a priori estimate

$$\hat{x}_k^+ = \hat{x}_k^- + K_k (y_k - H_k \hat{x}_k^-) =$$

a posteriori state estimate

$$P_k^+ = (I - K_k H_k) P_k^- (I - K_k H_k)^T + K_k R_k K_k^T$$

Where  $\hat{x}_k^+$ ,  $P_k^+$ ,  $\hat{x}_k^-$ ,  $P_k^-$  are a posteriori estimate, a posteriori covariance, a priori estimate, a priori covariance.

### 4.6.3. Extended Kalman Filter

Extended Kalman Filter is the nonlinear version of the Kalman filter which linearizes about the current mean and covariance. Linearization is carried out by means of partial derivatives of nonlinear state functions or their Taylor series expansion. Assuming that a nonlinear system is being represented as differentiable functions:

$$x_k = f(x_{k-1}, u_{k-1}) + w_{k-1}$$

$$y_k = h(x_k) + v_k$$

The function  $f$  can be used to compute the predicted state from the previous estimate and similarly the function  $h$  can be used to compute the predicted measurement from the predicted state. However,  $f$  and  $h$  cannot be applied to the covariance directly. Instead a matrix of partial derivatives (the Jacobian matrix) is computed.

#### 4.6.4. Unscented Kalman Filter

When the state transition and observation models are highly non-linear, the extended Kalman filter can give particularly poor performance. The biggest problem with EKF are[5]:

1. Linearization can produce highly unstable filters if the assumptions of local linearity is violated.
2. the derivation of the Jakobian matrices is nontrivial in most applications and often lead to significant implementation difficulties.

Unscented Kalman Filter is using Unscented transform to transform state vector into a set of weighted Sigma Points, because it is easier to estimate a distribution than a nonlinear function[5].

The biggest advantages of UKF are:

1. No need of linearization.
2. No need for calculation of the Jakobian matrices.

At the moment UKF is the best filter for nonlinear tracking state estimation, because of the best trade-off between precision and computational complexity.

## 5. Navigation

### 5.1. Overview

In this section methods and algorithms of navigation will be described.

Navigation understood as a decision in which direction UAV should move to meet mission.

### 5.2. Missile guidance laws

Guidance approaches [4] originate from the military applications and precision guided weapons. The guidance was understood as the strategy for steering the missile to intercept, while control was treated as the tactics of using missile actuators to implement the strategy. Therefore guidance is a strategy aimed at targeting a certain position that can vary other time. Most fundamental guidance laws include:

- Velocity Pursuit
- Proportional Navigation
- Command-to-Line-of-Sight
- Beam Riding

Velocity pursuit guidance is based on the idea, that the missile should always head for the target's current position. To implement this strategy the required information is the bearing to the target and the current direction of the vehicle. However, the law is characterized by high lateral acceleration demanded, often infinitely nearby the target position. Therefore it is not suitable for adaptation for UAV navigation.

Proportional navigation assumes, that the missile should keep a constant bearing to the target during the whole flight, therefore the change in the vehicle direction is induced by the change in bearing. The lateral acceleration is given by:

$$n_m = \alpha v_c \dot{\phi}$$

In the augmented version of this guidance law the vehicle also tries to compensate for the target acceleration:

$$n_m = \alpha \left( v_c \dot{\phi} + \frac{1}{2} n_t \right)$$

The proportional navigation laws are often used as the reference for more advanced approaches.

The missile should stay on the straight line from the launcher to the target throughout the trajectory is the underlying assumption of the Command-to-Line-of-Sight and Beam Riding laws:

$$n_m = 2 \frac{v_m v_t}{d} \beta$$

where  $\beta$  is tabularized non-linear acceleration factor depending on missile and vehicles directions and  $d$  is the distance between target and launch position.

### 5.3. Linear proportional–integral–derivative controller (PID) trajectory tracking

A PID controller is a commonly adopted method in feedback control. Despite the dynamic nature of the fixed-wing aircraft flight, the linear controller used on the cross-track error (the lateral deviation from a desired trajectory) provides surprisingly good performance on a straight line tracking task. The desired lateral acceleration is specified by the formula:

$$n_m(t) = K_p e(t) + K_i \int_0^t e(\tau) d\tau + K_d \frac{d}{dt} e(t)$$

where  $e(t)$  is cross-track error, and  $K_p$ ,  $K_i$ ,  $K_d$  are the proportional gain, the integral gain and the derivative gain – the tuning parameters of the controller.

In this controller, the proportional term is accompanied by integral and derivative terms. The integral term accumulates the error over time, providing enhanced control using the historical data. The derivative term predicts the error using the linear extrapolation, providing enhanced control using anticipative abilities.

Although simple in principle, the optimal parameter tuning of PID controller parameters is a non-trivial problem. Multiple methods have been described in literature [3, 7] ranging from manual tuning by an experienced professional, through heuristic analytic methods like Ziegler-Nichols method, to experimentation based tuning using specialized optimization software.

### 5.4. Non-linear guidance logic for trajectory tracking

Park et al. [12] presented a nonlinear guidance logic for trajectory tracking. Their method was motivated by the proportional navigation for missile guidance from Section 5.2, which is the most preferred approach to guidance. In order to overcome the limitation of feedback control in following curved paths, they extend their guidance logic with an anticipatory element.

$$n_m = 2 \frac{V^2}{L_1} \sin \eta$$

Two properties define the behaviour of this guidance law:

1. The direction of the acceleration is determined by the sign of the angle between aircraft and reference point line-of-sight and the aircraft orientation.
2. A circular path is defined unambiguously by the aircraft position and orientation and the position of the reference point. As  $L_1 = 2R \sin \eta$ , the acceleration produced by the guidance law is in fact the centripetal acceleration required to stay on this circular path, since

$$a_{centripetal} = \frac{V^2}{R} = 2 \frac{V^2}{L_1} \sin \eta = n_m.$$

The angle of approach to the desired path produced by the resulting logic is large, when vehicle is far from the desired path and small, if it is nearby.

The simulations and flight experiments have shown, that nonlinear guidance performs similarly well to proportional-derivative controller, when following a straight line. For the curved trajectory in no wind and wind conditions, the anticipatory element of  $L_1$  look-ahead distance and usage of ground speed for calculating the lateral acceleration enabled the nonlinear controller to tightly follow the trajectory, while the linear controllers failed.

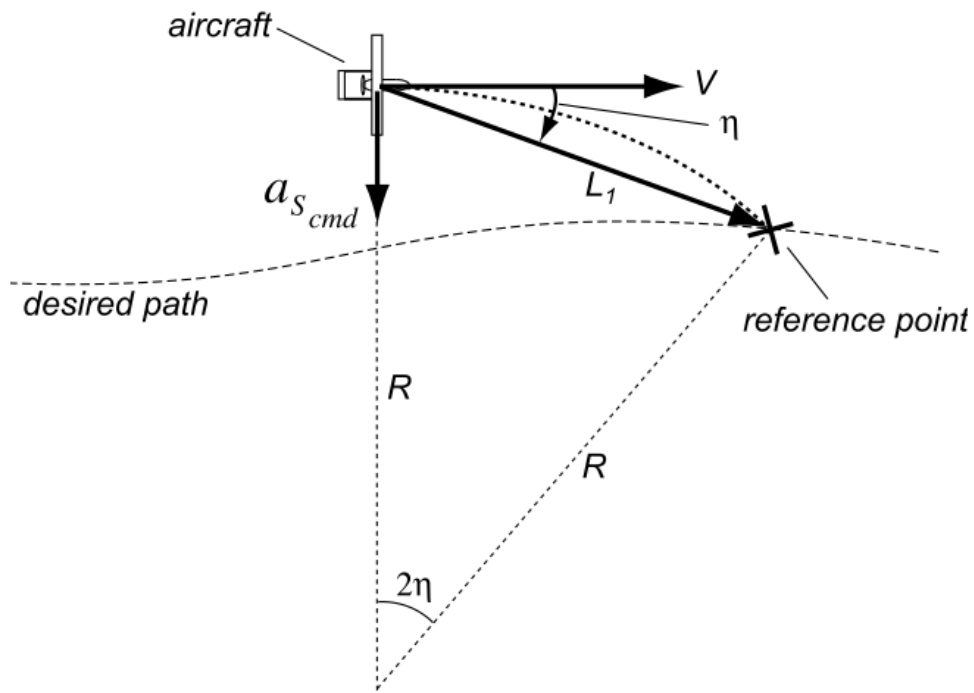


Figure 15: Diagram for nonlinear guidance logic (after [12])

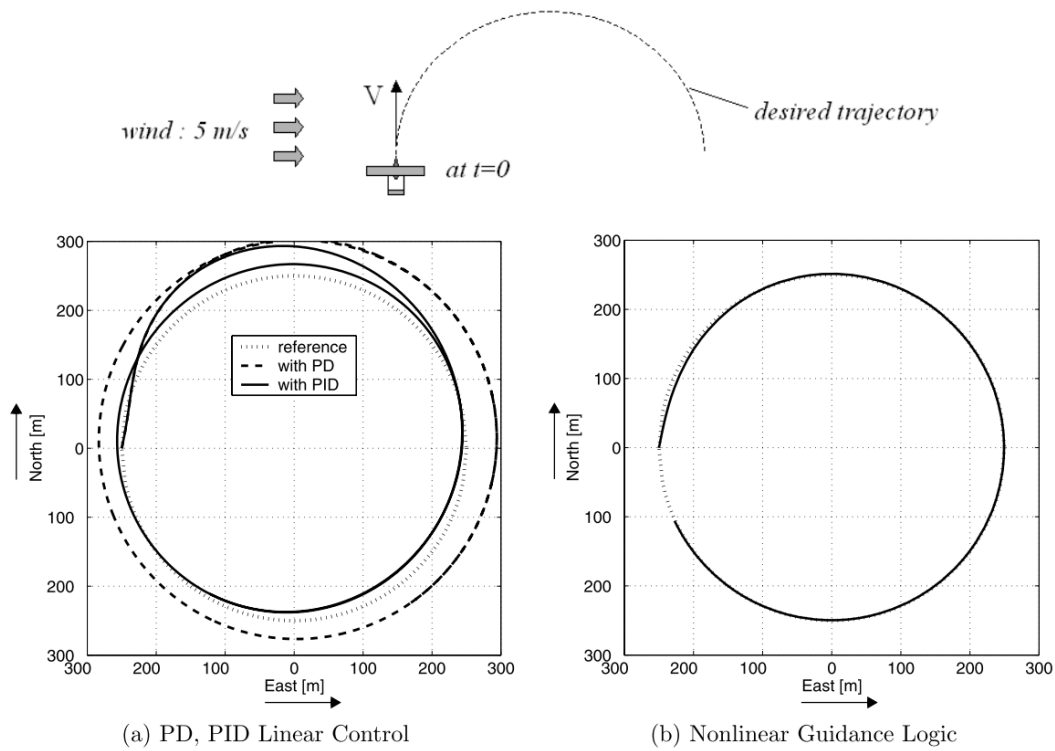


Figure 16: Curved line following with wind - comparison of linear and nonlinear controllers (after [12])

## 6. Future work

In this work all layers from physical to the navigation layer have been described – from the design of the mechanics through control, localization and navigation. After consultations with end users, we have created a draft design of these components of the UAV.

Based on research conducted for creating this document all elements will be implemented and evaluated in laboratory environment, later a design of the prototype will be created and described in deliverable 2.8. After positive feedback from end users and reviewers implementation of the prototype will start. In deliverable 2.9 results of tests of the system will be described.

Some interesting research areas haven't been described in this document (e.g. obstacle avoidance), because they are complex problems and their priority is low. If there is enough time development in these areas will be described in the following deliverables.

## Conclusions

In this document proposed algorithms for UAV control and navigation have been described. As well as UAV design and requirements which led us to these design decisions.

Mechanically a lightweight electrically powered UAV design has been presented. It is very stable and has an exchangeable gimbal. Also possible launch systems have been presented.

Control algorithms have been presented with equations of motion - necessary to understand how to describe UAV motion. Also methodology for designing a PID controller has been described. It is the oldest, but also the most widespread, and computationally optimal method for control system.

Localization sensors and their reliability have been presented as well as Kalman Filter - a method to combine all these measures into a single reliable state have been described in this section.

Concluding, based on this research an autonomous UAV can be built as well as its algorithms.



## References

- [1] Honeywell Aerospace. Gg1320an digital laser gyro leaflet.
- [2] Honeywell Aerospace. Gg5300 leaflet.
- [3] Karl Johan Astrom and Richard M. Murray. *Feedback Systems*. Princeton University Press, 2009.
- [4] Erik Berglund. *Guidance and control technology*, 2001.
- [5] Simon J. Julier and Jeffrey K. Uhlmann. A new extension of the kalman filter to nonlinear systems. 1997.
- [6] Elliott D Kaplan and Christopher J Hegarty. *Understanding GPS: principles and applications - 2nd ed*. Artech House mobile communications library. Artech House, Norwood, MA, 2006.
- [7] Y. Li, K.H. Ang, and G.C.Y. Chong. PID control system analysis and design. *IEEE Control Systems Magazine*, 2006.
- [8] Sergiusz Łuczak. Pomiary odchylenia od pionu z użyciem akcelerometrów mems. *Pomiary Automatyka Robotyka*, 2008.
- [9] Rudy Negenborn. Robot localization and kalman filters. Master's thesis, UTRECHT UNIVERSITY, 2003.
- [10] NOAA/NGDC and CIRES. Us/uk world magnetic model – epoch 2010.0.
- [11] NOAA/NGDC and CIRES. Us/uk world magnetic model us/uk world magnetic model – epoch 2010.0 main field total intensity.
- [12] S. Park, J. Deyst, and J.P. How. A new nonlinear guidance logic for trajectory tracking. In *Proceedings of the AIAA Guidance, Navigation and Control Conference*, 2004.
- [13] Dan Simon. *Optimal State Estimation: Kalman, H Infinity, and Nonlinear Approaches*. John Wiley & Sons, 2006.
- [14] Brian L. Stevens and Frank L. Lewis. *Aircraft Control and Simulation*. Wiley, New York :, 1992.
- [15] David H Titterton and John L Weston. *Strapdown Inertial Navigation Technology (2nd Edition)*. Institution of Engineering and Technology, 2004.
- [16] Jean-Marie Zogg. Gps. essentials of satellite navigation. compendium. 2009.



# Attachment no.1



**Intelligent Information System Supporting  
Observation, Searching and Detection for  
Security of Citizens in Urban Environment**



*European Seventh Framework Programme  
FP7-218086-Collaborative Project*

## Title: User Scenario

**Scenario No:**

**Scenario Title:**

**Person responsible (name, e-mail):**

**People involved:**

The content of the scenario before the implementation of new tools listed below	.....
Lacks (needs)	<ul style="list-style-type: none"> <li>• ...</li> <li>• ...</li> </ul>
List of solutions (tools) to deal with a problem	<ul style="list-style-type: none"> <li>• ...</li> <li>• ...</li> </ul>
The content of the scenario after the implementation of new tools listed above	.....



This project is funded under 7<sup>th</sup> Framework Program



**Intelligent Information System Supporting  
Observation, Searching and Detection for  
Security of Citizens in Urban Environment**



*European Seventh Framework Programme  
FP7-218086-Collaborative Project*

## **Tactical and Technical Requirements**

**Element No.:**

**Element Name:**

### **1. General description**

## 2. Element's features

### 2.1 Table of features

Feature No.	Feature name	Priority	Added by	Scenario No.

**F.X.Y** where **X** is the number of the element and **Y** is the number of feature.

**Priority 1** – essential, **2** –optional, **3** – extras

**Scenario No. Y-X** where **Y** is **NI** – Northern Ireland or **P** – Poland, **X** – scenario number

### 2.2 Features description

-

### 3. Technical data

Technical Data No.	Parameter	Value	Added by	Scenario No.

### 4. Suggestions

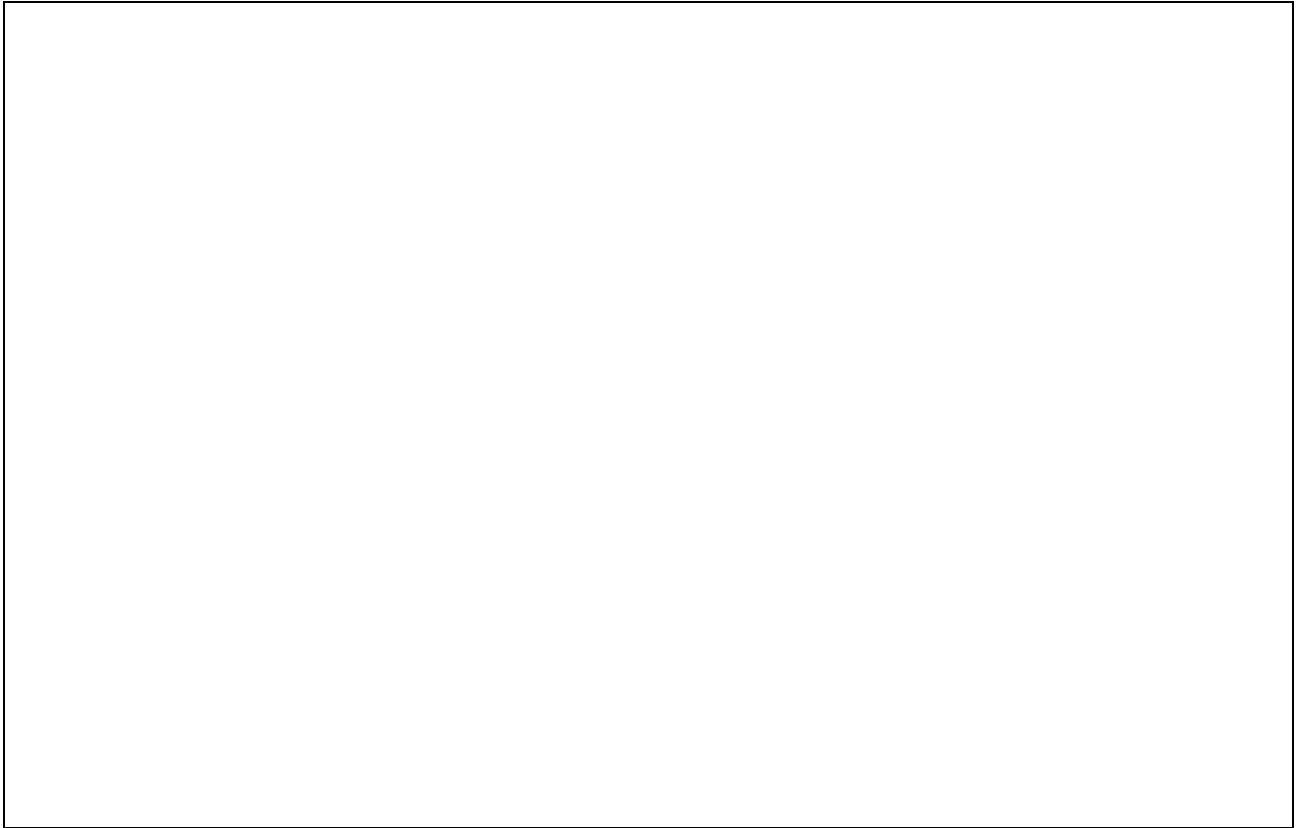
#### 4.1 Table of suggestions

Suggestion No.	Suggestion	Added by

#### 4.2 Suggestion description (optional)

-

## 5. Summary



This project is funded under 7<sup>th</sup> Framework Program

Version	Date	Updates and revision history	Editor
0.1	09/03/2010	Document template	Grzegorz Sobański, PUT
0.11	30/03/2010	ToC draft	Paweł Lubarski, PUT
1.0	14/06/2010	Stable version for reviews	Paweł Lubarski, PUT